

Fluctuation of the Ca^{2+} -sequestering activity of permeabilized sea urchin embryos during the cell cycle

(dielectric breakdown/mitosis)

FRANK A. SUPRYNOWICZ* AND DANIEL MAZIA

Department of Biological Sciences, Stanford University, Hopkins Marine Station, Pacific Grove, CA 93950; and Department of Zoology, University of California, Berkeley, CA 94720

Contributed by Daniel Mazia, December 6, 1984

ABSTRACT We have followed the sequestration of Ca^{2+} by intracellular compartments in sea urchin embryos through the first cell cycles. To gain biochemical access to these compartments, the embryos were permeabilized by brief exposure to an intense electric field. Sequestration was determined as the retention of tracer, ^{45}Ca , after filtration of aliquots on Millipore filters. The permeabilized cells sequester Ca^{2+} at a constant rate for at least 20 min, with the following characteristics: (i) ATP is required. (ii) Sequestration occurs at Ca^{2+} levels corresponding to those estimated *in vivo*. (iii) The Ca^{2+} concentration dependence of sequestration and its insensitivity to mitochondrial poisons imply that the activity derives from a single, nonmitochondrial transport system. The Ca^{2+} -sequestering activities of embryos that are permeabilized at successive stages of the first cell cycle (one-cell stage) progressively increase to 5 times the initial level. The rate of sequestration is maximal during telophase and, in some populations of zygotes, is nearly as great throughout prophase. Over the course of the second cell cycle (two-cell stage), the activity undergoes a 2-fold oscillation that bears the same temporal relationship to mitosis as the previous fluctuation.

The hypothesis that cytosolic Ca^{2+} levels undergo cyclical fluctuation during the cell cycle has been put forth to account for a variety of events. A local increase in Ca^{2+} may regulate the poleward migration of chromosomes via the disassembly of spindle microtubules (see refs. 1 and 2; reviewed in ref. 3). There is evidence that the transition from metaphase to anaphase is triggered by changing concentrations of intracellular Ca^{2+} (4-6). The inactivation of a protein responsible for arresting cells in meiotic metaphase has been attributed to a transient increase in cytosolic Ca^{2+} (7, 8).

The abundant membranous components of the mitotic spindle (reviewed in ref. 9) are known to sequester Ca^{2+} *in vivo* (10) and *in vitro* (11). In many cells, the relative activity of a Ca^{2+} -activated ATPase, which appears to be associated with these membranes, differs during specific stages of the cell cycle (reviewed in ref. 12).

We anticipate that direct measurement of Ca^{2+} levels in living cells will, in the future, characterize or refute the proposed Ca^{2+} cycles. In the present work, we deal with oscillations in the activity of the Ca^{2+} -sequestering system of fertilized sea urchin eggs as they proceed through several cleavage divisions. The intracellular transport of Ca^{2+} is measured in embryos that have been permeabilized at successive stages of the cell cycle by brief administration of an intense electric field. Such treatment causes localized dielectric breakdown of the plasma membrane (13-16) without damaging intracellular membranes (13, 14).

MATERIALS AND METHODS

All manipulations were done at 18°C, unless otherwise indicated.

Handling of Gametes. Eggs and sperm were obtained from the sea urchin *Lytechinus pictus*, after intracoelomic injection of 0.5 M KCl. Sperm was collected dry at 4°C. Eggs were shed into natural seawater, concentrated by brief centrifugation at $1000 \times g$, and resuspended in HCl/seawater, pH 5, to dissolve the jelly layer. After 3 min, they were transferred to beakers of natural seawater and were maintained in suspension by gentle stirring. Suspensions were fertilized by introducing a few drops of dilute sperm. Egg density is defined as the volume fraction of a suspension that is occupied by packed unfertilized eggs.

Solutions. Except where noted, embryos were permeabilized (see below) in Ca^{2+} sequestration medium (CaS medium): 250 mM K gluconate/250 mM *n*-methylglucamine (Sigma)/50 mM Hepes/5 mM NaCl/5 mM oxalic acid/2 mM disodium EDTA, plus sufficient MgSO_4 and CaCl_2 for 1 mM free Mg^{2+} and 1-10 μM free Ca^{2+} (Table 1). The solution is titrated to pH 7.2 by addition of glacial acetic acid (≈ 190 mM acetate). CaS medium is osmotically equivalent to sea urchin cytoplasm, and it approximates normal intracellular concentrations of K^+ , Na^+ , H^+ , and Cl^- (20-22).

Permeabilization. The permeabilization chamber was made by sealing two stainless steel plates across the open sides of a U-shaped piece of Plexiglas, such that two walls of the chamber become stainless steel electrodes that are spaced 1 cm apart. The internal dimensions of the chamber are $6 \times 2 \times 1$ cm.

Fertilized eggs (inside fertilization membranes) were collected by brief centrifugation (see above), washed with >50 vol of Ca^{2+} -free seawater (460 mM NaCl/10 mM KCl/27 mM MgCl_2 /29 mM MgSO_4 /5 mM Hepes-NaOH, pH 7.8), then with >50 vol of CaS medium, and finally were resuspended to a population density of $<1.5\%$ in CaS medium. A 6.1-ml sample of suspension was transferred to the permeabilization chamber and was shocked by discharging a 10 μF capacitor that had been charged to 1500 V by means of an electrophoresis power supply. Under these conditions, the embryos initially experience an electric field of 1500 V/cm, which decreases exponentially to $1/e$ of this value over 100 μsec . Each electric shock produces 2 pores in the plasma membrane (13). Two additional pores may be induced by a second shock, applied after the suspension is agitated to reorient the cells with respect to the electrodes (13). Having found that the sequestration of Ca^{2+} is optimal in zygotes with 20 pores (Fig. 1), we applied 10 shocks in our routine procedure. Polarization of the electrodes was prevented by reversing their polarity after each capacitor discharge.

The publication costs of this article were defrayed in part by page charge payment. This article must therefore be hereby marked "advertisement" in accordance with 18 U.S.C. §1734 solely to indicate this fact.

*Present address: Department of Cell Biology and Anatomy, Johns Hopkins University School of Medicine, Baltimore, MD 21205.

Table 1. Composition of Ca²⁺ buffers

Ca ²⁺ , μM	CaCl ₂ , μM	MgSO ₄ , mM	⁴⁵ CaCl ₂ , μCi/ml
10.0	944	5.95	30
3.0	402	6.45	20
2.0	285	6.56	20
1.0	153	6.69	15

Concentrations of free Ca²⁺ and Mg²⁺ were calculated as described by Blinks *et al.* (17), using stability constants from Martell and Smith (18). We take into account the binding of H⁺, Ca²⁺, and Mg²⁺ to EDTA, gluconate, oxalate, acetate, and ATP. The reader is referred elsewhere (19) for a more complete discussion. ⁴⁵CaCl₂ was from New England Nuclear (23–34 mCi per mg of Ca; 1 Ci = 37 GBq).

The dye 6-carboxyfluorescein readily enters permeabilized embryos but is excluded by intact ones. We have used this probe to determine that our protocol permeabilizes 100% of the embryos in a suspension and to ascertain that these remain permeable for at least 25 min (data not shown). A more detailed description of the permeabilization technique appears elsewhere (19).

Measurement of Sequestration. Aliquots of suspensions of permeabilized embryos were mixed with equal volumes of CaS medium (containing 2× the final concentration of ⁴⁵Ca shown in Table 1) in 20-ml glass vials that had been treated with Sigmacote (Sigma). Rotary shaking was used to maintain uniform suspension. Sequestration was initiated (after 2 min) by addition of MgATP to a final concentration of 2 mM.

Millipore filters (0.22-μm pore; type MF) were placed in 25-mm Nuclepore Swin-Lok holders that were machined as to expose one face of the filter and create a reservoir for washes (19). The holders were connected to a vacuum, and the filters were wetted with CaS medium just before use. ⁴⁵Ca accumulation was monitored by spotting duplicate 0.4-ml aliquots from the incubating suspensions onto filters, and immediately washing each with four 1-ml volumes of ice-cold CaS medium. This regime lowers the radioactivity retained by the filters to a stable plateau (data not shown). Each filter then was immersed in 5 ml Beta-Blend (West-Chem Products, San Diego, CA) and was analyzed 2 hr later in a Beckman LS-8000 liquid scintillation counter.

An additional aliquot of each incubation was sonicated for 30 sec (Branson Sonifier) and was assayed for protein by the method of Bradford (23), with bovine serum albumin as standard. Rates of sequestration are expressed as nmol of Ca

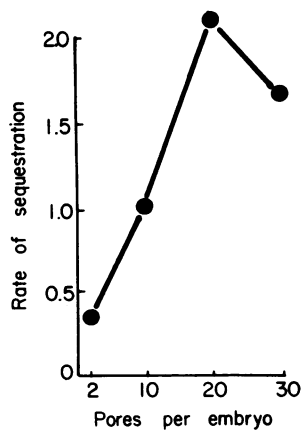


FIG. 1. What number of electrically induced pores is optimal for Ca²⁺ sequestration? Ten minutes after fertilization, aliquots from a suspension of embryos were given 1, 5, 10, or 15 electric shocks to induce 2, 10, 20, or 30 pores in their plasma membrane. Rates of sequestration were calculated from the increase in ⁴⁵Ca retained on Millipore filters over 11 min (10 μM Ca²⁺).

retained by the Millipore filters per min per mg of total egg protein.

RESULTS

Characteristics of Sequestration. In the presence of ATP, permeabilized embryos sequester Ca²⁺ at a constant rate for at least 20 min. The activity is not affected by inhibitors of the uptake of Ca²⁺ by mitochondria (Fig. 2).

Ca²⁺ does not accumulate in the absence of ATP and the nonfilterable ⁴⁵Ca in this case probably represents ATP-independent Ca²⁺ binding to membranes, proteins, etc. Such an interpretation is supported by the observation that ATP-dependent Ca²⁺ accumulation extrapolates to an identical initial value (Fig. 2).

Apparently, the mitochondria of permeabilized embryos produce sufficient ATP to fuel a low level of Ca²⁺ sequestration by other intracellular compartments, because some ⁴⁵Ca accumulates in the absence of a preexisting pool of ATP (incubation with 2 mg of apyrase per ml), so long as mitochondria are not poisoned (Fig. 2).

The Ca²⁺ concentration dependence of sequestration obeys Michaelis–Menten kinetics (Fig. 3A), suggesting that a single transport enzyme is responsible. A double reciprocal plot of the data (Fig. 3B) indicates that uptake is 50% active at 2.8 μM Ca²⁺ and predicts a threshold for sequestration (5% activity) at 0.1 μM Ca²⁺. This threshold is similar to recent measurements of resting cytosolic Ca²⁺ in a variety of cells (24–29), including estimates in sea urchin eggs (30). We have observed an almost identical Ca²⁺ dependence for sequestration in unfractionated homogenates of *Strongylocentrotus purpuratus* embryos (ref. 19; unpublished observations).

Intactness of Permeabilized Embryos. Because permeabilized zygotes sequester Ca²⁺ at a slower rate than do homogenized ones (Fig. 4), we have asked whether the electric shocks damage their sequestering system by comparing Ca²⁺ transport in homogenates prepared from permeabilized and intact (not permeabilized) embryos. These activities are very similar (Fig. 4), suggesting that the permeabilization procedure has not damaged those elements ultimately responsible for the sequestration of Ca²⁺.

The fertilization membrane does not exclude ions and small molecules (*M_r* < 1000) and, therefore, is not expected

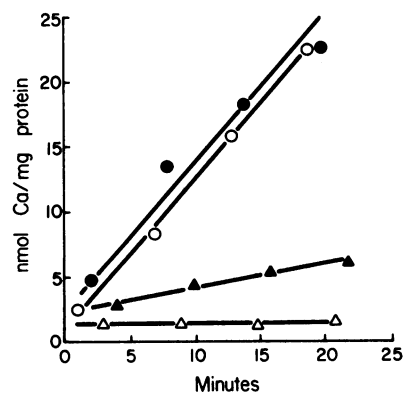


FIG. 2. Sequestration requires ATP and (at 2 μM Ca²⁺) does not include mitochondrial uptake. Seventy-five minutes after fertilization, embryos were permeabilized, divided into four portions, and mixed with ⁴⁵Ca-containing CaS medium (2 μM Ca²⁺). Apyrase (2 mg/ml) was immediately added to two portions (▲ and △); the other two portions received 2 mM MgATP 2 min later (● and ○). ○ and △ contained inhibitors of mitochondrial Ca²⁺ transport: 10 μM FCCP (carbonylcyanide *p*-trifluoromethoxyphenylhydrazone) and 20 μg of oligomycin per ml (Sigma). Apyrase (7 units of ATPase per mg) was purchased from Sigma. One unit of activity liberates 1.0 μmol of P_i per min at pH 6.5 at 30°C.

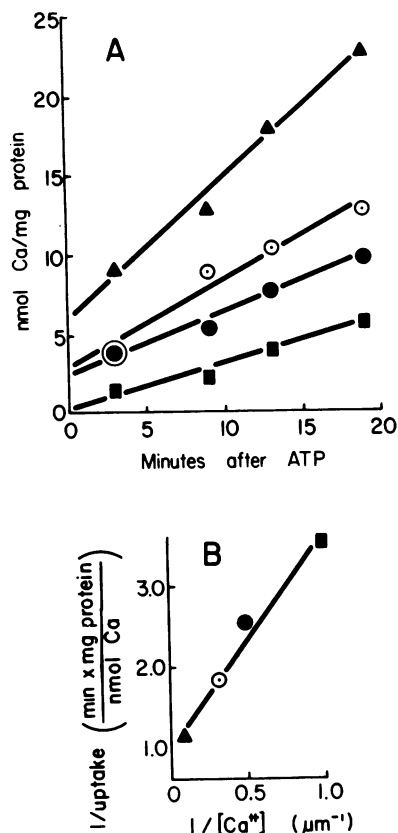


FIG. 3. Ca^{2+} concentration dependence of sequestration. Embryos were permeabilized 13 min after fertilization ($1 \mu\text{M}$ Ca^{2+}). Aliquots of the suspension were mixed 1:1 with CaS medium formulations that contained ^{45}Ca and appropriate concentrations of CaCl_2 and MgSO_4 to give 1 mM Mg^{2+} and 1 (\blacksquare), 2 (\bullet), 3 (\circ), or 10 (\blacktriangle) μM Ca^{2+} after mixing. Rates of uptake in B are determined by linear regression analysis of data in A. $K_m = 2.8 \times 10^{-6}$ M Ca^{2+} ; $V_{\text{max}} = 1.0$ nmol of Ca/(min \times mg of protein).

to undergo dielectric breakdown in an electric field. Rather, it should remain intact and confine macromolecules that may leak through the permeabilized plasma membrane. Analysis of cell-free supernatants from a permeabilized suspension in-

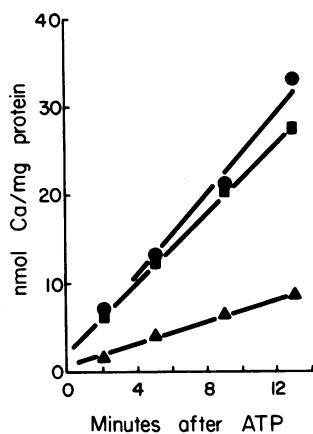


FIG. 4. The permeabilization protocol does not functionally damage the Ca^{2+} -sequestering system. Embryos were washed and resuspended in CaS medium ($2 \mu\text{M}$ Ca^{2+}) 75 min after fertilization. One-third of the suspension was homogenized (glass, Dounce-type homogenizer), and 2/3 was permeabilized. One-half of the permeabilized suspension then was homogenized. ^{45}Ca and ATP were added to all three suspensions, and sequestration was monitored. Permeabilized embryos (\blacktriangle) sequester Ca^{2+} 27% as rapidly as homogenized ones (\bullet), while those that are homogenized after permeabilization (\blacksquare) are 84% as active as the control.

indicates that the fertilization membrane retains >97% of total egg protein for at least 20 min after permeabilization (data not shown).

Diffusion of Calcium into Permeabilized Embryos. As described, we routinely incubated permeabilized embryos with ^{45}Ca containing CaS medium for 2 min before adding ATP. That Ca^{2+} equilibrates between the medium and cytosol within this period is shown by incubating permeabilized suspensions with ^{45}Ca for 2, 5, and 10 min. As Fig. 5 illustrates, all three incubations result in nearly identical rates of sequestration, implying that Ca^{2+} has equilibrated within 2 min.

Ca^{2+} equilibrium largely is maintained during sequestration, because external calcium enters permeabilized embryos approximately as rapidly as it is compartmentalized. We measured rates of sequestration in media in which the Ca/EDTA ratio remained constant, while the concentration of both varied 20-fold. In this way, the rate at which calcium entered the permeabilized zygotes increased 20-fold. In response, sequestration was stimulated only 1.7-fold (data not shown). Together with the results of Fig. 5, this experiment suggests that the concentration of Ca^{2+} near the sequestering compartments of permeabilized embryos is very similar to that of the medium throughout our experiments.

Sequestration Activity During the Cell Cycle. Whereas the rate at which Ca^{2+} is sequestered in permeabilized embryos is constant for at least 20 min after permeabilization (see above), the activities of embryos that are permeabilized at different stages of the cell cycle are not identical. (The mitotic stages to which we now refer were identified by microscopic observation of fixed samples, as described in the legend to Fig. 6.)

Over the course of the first cell cycle (one-cell stage), the rate of sequestration (measured without oxalate at 1 or 2 μM Ca^{2+}) increases 5-fold. It is maximal during telophase (Figs. 6 and 7) and, in some populations of zygotes, is nearly as great throughout prophase (Fig. 6). During the second cell cycle (two-cell stage), the activity undergoes a 2-fold oscillation that bears the same temporal relationship to mitosis as the previous fluctuation (Figs. 6 and 7). Because of asynchrony in the population, these changes are likely to occur more rapidly and to be of greater magnitude in individual embryos.

DISCUSSION

If cell cycles include cycles of Ca^{2+} concentration in the cytoplasm, we might expect to find cyclical changes in the ac-

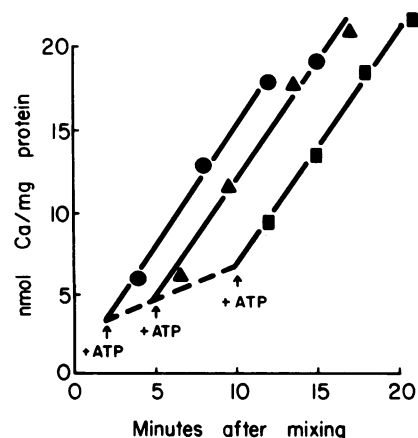


FIG. 5. Equilibration of Ca^{2+} across the plasma membrane after permeabilization. Seventy minutes after fertilization, embryos were permeabilized and incubated with ^{45}Ca for 2 (\bullet), 5 (\blacktriangle), or 10 (\blacksquare) min before 2 mM MgATP was added to initiate Ca^{2+} uptake ($2 \mu\text{M}$ Ca^{2+}). Broken line represents sequestration that is supported by endogenous ATP (cf. Fig. 2).

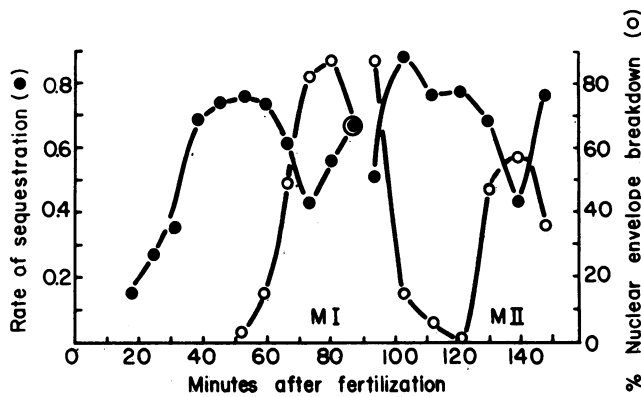


FIG. 6. Ca^{2+} sequestration in embryos permeabilized at successive stages of the first two cell cycles. An aliquot of embryo suspension was permeabilized every 7 or 9 min, and its Ca^{2+} -sequestering activity was measured immediately (without oxalate) at $2 \mu\text{M}$ Ca^{2+} . [When oxalate is omitted, 1.88 mM less MgSO_4 is used in the CaS medium formulations (Table 1).] At the same time, additional aliquots of intact (not permeabilized) embryos were fixed in ethanol/acetic acid (3:1), to quantitate breakdown of the nuclear envelope with Nomarski optics, or to observe phase-contrast images of condensed chromosomes after staining with orcein. Rates of sequestration are determined from the difference in triplicate Millipore filtrations performed 12 min apart. Two experiments are shown. MI, first mitosis (73 min, metaphase; 80 min; anaphase; 87 min, telophase); MII, second mitosis. Embryonic development and measurements of Ca^{2+} transport took place at 18°C .

tivity of the system by which Ca is sequestered. The Ca^{2+} -sequestering system in sea urchin eggs is known from studies on live embryos (10) and isolated mitotic spindles (11), and it has been visualized cytochemically at the electron microscopic level (31). We have characterized it in some detail in homogenates (19) in a study that will be published elsewhere.

Turning to permeabilized cells for a more realistic look at a process that cannot yet be measured in living cells, we find that the maximum rates of sequestration of Ca^{2+} are lower than those given by homogenates, by a factor of 4. Two possible criticisms of the permeabilized system are eliminated. (i) The experiment illustrated in Fig. 4 shows that the permeabilization procedure has not damaged the sequestration mechanism itself. (ii) The experiment illustrated in Fig. 5 shows that the permeabilization is adequate; the plasma membrane is no longer a barrier to equilibrium between in-

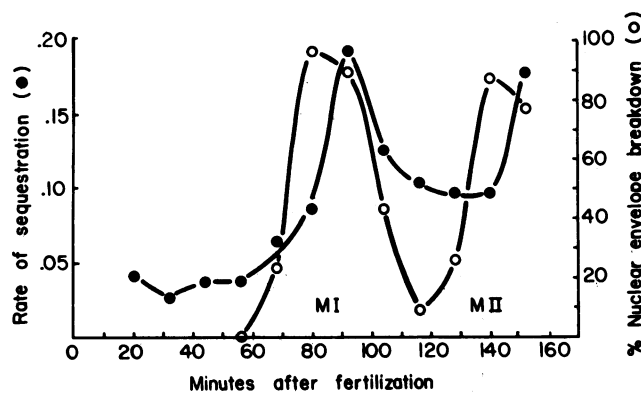


FIG. 7. Ca^{2+} sequestration in embryos permeabilized at successive stages of the first two cell cycles. An aliquot of embryo suspension was permeabilized every 12 min and, as described in Fig. 6, was assayed for Ca^{2+} -sequestering activity in the presence of $1 \mu\text{M}$ Ca^{2+} (no oxalate). Embryonic development and measurements of Ca^{2+} transport took place at 16°C .

tracellular and extracellular Ca^{2+} .

The permeabilized cells may well be preserving molecular or structural factors that regulate sequestration in the living cell. It is worth recalling that we retain nearly all diffusible macromolecules by permeabilizing embryos within their fertilization envelopes. These envelopes allow the free passage of ions and small molecules but not of macromolecules that would be highly diluted by homogenization.

Structural changes of the Ca-sequestering system during the cell cycle have been discussed by a number of authors who propose (9, 32, 33), with some evidence (10, 11, 34, 35), that the system is concentrated in the very abundant membranes of the mitotic apparatus. The cycles of sequestering activity in our permeabilized cells could be influenced by the changing disposition of Ca-sequestering membranes during interphase and mitosis.

Consistently, a peak in the rate of Ca^{2+} sequestration is observed shortly after peak breakdown of the nuclear envelope (mitotic telophase). In contrast, uptake is relatively inactive at metaphase (Figs. 6 and 7). In some populations of embryos, a second peak of sequestering activity coincides with prophase. This peak decreases concomitant with the onset of nuclear envelope breakdown (Fig. 6). It may be significant that these relative maxima of Ca^{2+} sequestration are seen at times when immunofluorescence studies show the largest arrays of astral microtubules (36, 37). The size of the mitotic asters increases throughout anaphase and is greatest during telophase. The "streak stage," or "interphase aster" of the first cell cycle (one-cell stage) reaches maximal proportions during prophase.

Since our method measures the net accumulation of tracer ^{45}Ca , changing rates of accumulation may reflect fluctuations in the rate at which Ca^{2+} is sequestered or released. The degree to which release influences rates of accumulation depends on the dilution of sequestered tracer by ^{40}Ca inside the sequestering compartments.

In the presence of 5 mM oxalate (cf. Figs. 1-5), ^{45}Ca is released at only 5% of the rate at which it accumulates (unpublished data); thus, we selectively measure sequestration. We have determined rates of accumulation throughout the cell cycle without using oxalate (Figs. 6 and 7) in order to approximate more closely conditions within the living embryo. Under these conditions, tracer is released 21%-38% as rapidly as it accumulates. This variation in the rate of release, however, does not explain most of the fluctuation in the rate of accumulation, and the latter truly can be called a sequestration cycle (unpublished data). The observation that oxalate greatly slows the rate at which tracer is released indicates that the active accumulation of Ca^{2+} by the sequestering compartments is working against an efflux that depends on the concentration of ionized Ca within the compartments.

The Ca^{2+} -sequestering activity that we describe may derive from the mitotic C-ATPase, which appears to be associated with intracellular membranes in a wide variety of organisms (reviewed in ref. 12). Both activities oscillate during the cell cycle and are most active during mitosis.

If there are cycles of Ca^{2+} concentration during cell cycles, they may be driven by changes in the activity of Ca^{2+} -sequestering systems. The main outcome of the present work is evidence that cell cycles can contain cycles of Ca^{2+} -sequestering activity. In the case of the sea urchin embryo, which does not grow, the cell cycles can be referred to as mitotic cycles. The permeabilization method gives access to the sequestering system for purposes of measurement and characterization. This method should be useful for studying other events that cannot be measured in living cells.

Note Added in Proof. Recently, Ca^{2+} sequestration has been described for an isolated cytoplasmic fraction in cultured mammalian cells and sea urchin embryos (38). Although the properties of this

system differ somewhat from those reported here, its activity undergoes a similar oscillation during the cell cycle.

We are grateful to Chris Patton for photography, illustrations, and construction of apparatus, and to Dr. David Epel for kindly sharing laboratory facilities. We thank Drs. M. Poenie and J. Zimmerberg for helpful discussions and Arlene Daniel for the preparation of this manuscript. Our study was supported by National Science Foundation Grant PCM-8104467. This work was submitted by F.A.S. in partial fulfillment of the requirements for the degree of Doctor of Philosophy at the University of California, Berkeley.

1. Cande, W. Z., McDonald, K. & Meeusen, R. L. (1981) *J. Cell Biol.* **88**, 618–629.
2. Cande, W. Z. (1982) *Cell* **28**, 15–22.
3. Inoué, S. (1981) *J. Cell Biol.* **91**, 131s–147s.
4. Izant, J. G. (1982) *J. Cell Biol.* **95**, 300 (abstr.).
5. Izant, J. G. (1983) *Chromosoma* **88**, 1–10.
6. Wolniak, S. M., Hepler, P. K. & Jackson, W. T. (1983) *J. Cell Biol.* **96**, 598–605.
7. Meyerhof, P. G. & Masui, Y. (1977) *Dev. Biol.* **61**, 214–229.
8. Newport, J. W. & Kirschner, M. W. (1984) *Cell* **37**, 731–742.
9. Paweletz, N. (1981) *Cell Biol. Int. Rep.* **5**, 323–336.
10. Kiehart, D. P. (1981) *J. Cell Biol.* **88**, 604–617.
11. Silver, R. B., Cole, R. D. & Cande, W. Z. (1980) *Cell* **19**, 505–516.
12. Petzelt, C. (1979) *Int. Rev. Cytol.* **60**, 53–92.
13. Knight, D. E. & Baker, P. F. (1982) *J. Membr. Biol.* **68**, 107–140.
14. Zimmermann, U., Pilwat, G. & Riemann, F. (1974) *Biophys. J.* **14**, 881–899.
15. Kinoshita, K., Jr., & Tsong, T. Y. (1977) *Proc. Natl. Acad. Sci. USA* **74**, 1923–1927.
16. Baker, P. F., Knight, D. E. & Whitaker, M. J. (1980) *Proc. R. Soc. London, Ser. B* **207**, 149–161.
17. Blinks, J. R., Wier, W. G., Hess, P. & Prendergast, F. G. (1982) *Prog. Biophys. Mol. Biol.* **40**, 1–114.
18. Martell, A. E. & Smith, R. M. (1974) *Critical Stability Constants* (Plenum, New York), Vols. 1–5.
19. Supryniewicz, F. A. (1984) Dissertation (Univ. of California, Berkeley).
20. Steinhardt, R. A., Lundin, L. & Mazia, D. (1971) *Proc. Natl. Acad. Sci. USA* **68**, 2426–2430.
21. Rothschild, L. & Barnes, H. (1953) *J. Exp. Biol.* **30**, 534–544.
22. Shen, S. S. & Steinhardt, R. A. (1978) *Nature (London)* **272**, 253–254.
23. Bradford, M. (1976) *Anal. Biochem.* **72**, 248–254.
24. Murphy, E., Coll, K., Rich, T. L. & Williamson, J. R. (1980) *J. Biol. Chem.* **255**, 6600–6608.
25. Baker, P. F. & Umbach, J. A. (1983) *J. Physiol. (London)* **341**, 61P.
26. Alvarez-Leefmans, F. J., Rink, T. J. & Tsien, R. Y. (1981) *J. Physiol. (London)* **315**, 531–548.
27. López, J. R., Alamo, L., Caputo, C., DiPolo, R. & Vergara, J. (1983) *Biophys. J.* **43**, 1–4.
28. Rink, T. J., Tsien, R. Y. & Warner, A. E. (1980) *Nature (London)* **283**, 658–660.
29. Ochs, D. L., Korenbrot, J. I. & Williams, J. A. (1983) *Biochem. Biophys. Res. Commun.* **117**, 122–128.
30. Epel, D., Patton, C., Wallace, R. W. & Cheung, W. Y. (1981) *Cell* **23**, 543–549.
31. Poenie, M., Patton, C. & Epel, D. (1983) *J. Cell Biol.* **97**, 181 (abstr.).
32. Harris, P. (1975) *Exp. Cell Res.* **94**, 409–425.
33. Harris, P. (1978) in *Cell Cycle Regulation*, eds. Jeter J. R., Cameron, I. L., Padilla, G. M. & Zimmerman, A. M. (Academic, New York), pp. 75–104.
34. Wolniak, S. M., Hepler, P. K. & Jackson, W. T. (1980) *J. Cell Biol.* **87**, 23–32.
35. Schatten, G., Schatten, H. & Simerly, C. (1982) *Cell Biol. Int. Rep.* **6**, 717–724.
36. Harris, P., Osborn, M. & Weber, K. (1980) *J. Cell Biol.* **84**, 668–679.
37. Balczon, R. & Schatten, G. (1983) *Cell Motil.* **3**, 213–226.
38. Petzelt, C. & Wülfroth, P. (1984) *Cell Biol. Int. Rep.* **8**, 823–840.